A. Supplementary Literature

A.1 Chapter 3—Kinematics of the Knee

Three translations and three rotations are required to describe the relative motion between two rigid bodies in three-dimensional space [35]. Therefore, considering the femur and tibia to be rigid, six variables are needed to describe knee kinematics. The coordinate system used to define the variables is presented, followed by a discussion of techniques used to measure these variables.

A.1.1 Joint Coordinate System

Knee kinematics are typically described in the literature using the Joint Coordinate System (JCS) proposed by Grood and Suntay [25]. This nonorthogonal coordinate system is defined by two bone-fixed axes and a unique floating axis (Figure A.1). Medial and lateral translations are measured along an axis that is fixed perpendicularly to the sagittal plane in the distal end of the femur. Usually, the intersection of this axis and the sagittal plane is set to correspond with the average center of rotation of the joint. Compression and distraction are measured along an axis that is fixed colinearly with the longitudinal axis of the tibia. Anterior and posterior translations are measured along a floating axis which is mutually perpendicular to the two fixed axes. Flexion and extension are measured about the femoral fixed axis, while internal and external rotation are measured about the tibial fixed axis. Abduction and adduction are measured about the floating axis.

When the tibial fixed axis is parallel to the femoral fixed axis, an infinite number of lines are mutually perpendicular to them. Hence, with this configuration, a unique floating axis can not be selected, and a singularity exists. In a practical sense, however, the fixed axes are unlikely to be parallel without severe trauma to the knee. Therefore, the singularity of the coordinate system is irrelevant to the description of moderate knee kinematics.

A.1.2 Kinematic Measurement Techniques

Except where noted, this section is based on the writing of Hefzy and Grood [30]. Researchers have used many methods to experimentally measure relative motion between the femur and tibia, including two-dimensional techniques, such as conventional roentgenograms. Three-dimensional techniques used by researchers to measure knee kinematics include high-speed photography, roentgen stereophotogrammetry, biplanar x-rays, electromagnetic devices, and external linkages. Robotics technology has also been adapted to measure knee kinematics [22]. However, the most popular kinematic measurement technique reported in the literature was one using an external linkage.

A.1.2.1 External Linkages

External linkages are mechanical systems for measuring joint kinematics. Three general classifications for these mechanisms exist: (a) planar linkages, (b) three-dimensional linkages, and (c) instrumented spatial linkages.

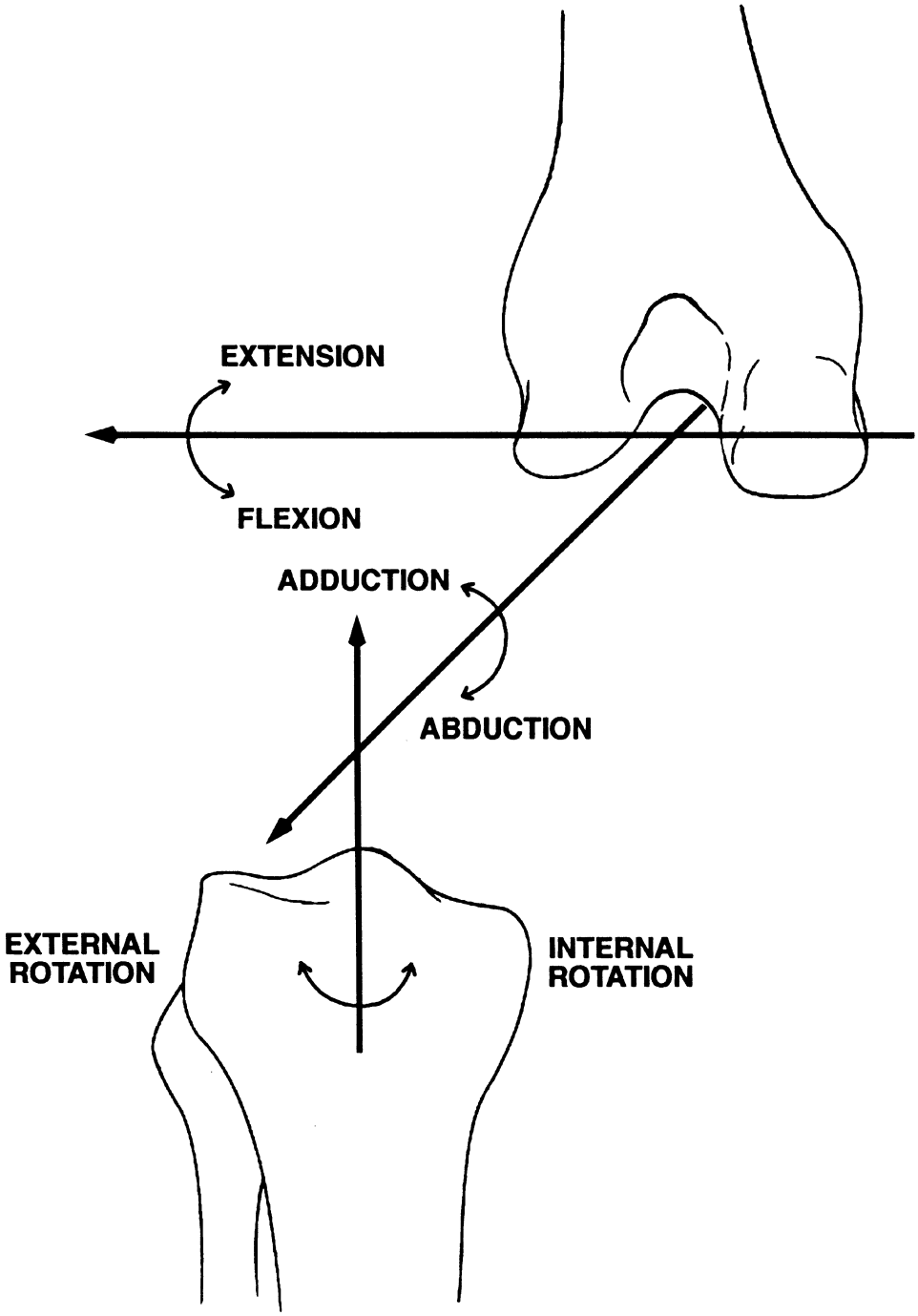

Figure A.1 Joint Coordinate System

A.1.2.1.1 Planar Linkages

A planar linkage can only measure motion in two dimensions. Because most joint motions are three-dimensional, their application is severely limited. To correctly measure the desired motion, a planar linkage must be manually aligned with the joint center of rotation. Large errors are introduced if the mechanism is not properly aligned.

A.1.2.1.2 Three-Dimensional Linkages

A three-dimensional linkage consists of three angular transducers aligned on mutually orthogonal axes. These mechanisms are limited because they can only measure rotations, and hence, not total joint motion. Furthermore, because the axes of the transducers are not always parallel to the axes of motion being measured, errors associated with cross-talk occur.

A.1.2.1.3 Instrumented Spatial Linkages

Instrumented spatial linkages are six degree-of-freedom mechanisms that measure total knee motion. One end of the linkage is fixed to the femur, and the other end is fixed to the tibia. The linkage consists of seven links connected in a series of one degree-of-freedom joints. A transducer at each joint indicates the relative motion of that joint. A matrix can be formulated to transform coordinates between systems attached to each link in a joint. Successive matrix multiplication yields a transformation matrix relating coordinate systems attached to the ends of the linkage. Including coordinate transformations between the linkage ends and the corresponding bones permits relative motion between the femur and tibia to be measured. Meglan [34] designed an instrumented spatial linkage consisting of a combination of a hinge, three rotational joints in a gyroscopic formation, a four bar linkage, and a sliding link to measure knee kinematics. Measurements using the linkage were reported to be within 0.5 mm for translations and 0.1° for rotations.

A.2 Chapter 4—Properties of Soft Tissues

Descriptive characteristics of soft tissues are organized in three categories: mechanics, biochemistry, and histology. Literature documenting previous areas of research within these categories is reviewed in the following section.

A.2.1 Mechanical Properties

Soft tissue specimens consist of bone-soft tissue-bone composites that exhibit viscoelastic behavior [27,56]. Structural properties, such as ultimate load and ultimate elongation, describe the behavior of the entire complex, while mechanical properties, including tangent modulus and ultimate strain, describe the behavior of the soft tissue itself [48,56]. Structural and mechanical properties are typically determined from a uniaxial tensile test of a specimen. The load-elongation curve establishes the structural properties: ultimate load, ultimate elongation, linear stiffness, and energy absorbed to failure (Figure A.2). The stress-strain curve establishes the mechanical properties: ultimate stress, ultimate strain, and tangent modulus (Figure A.3). Hence, in addition to the elongation and load applied to the specimen, the strain and cross-sectional area of the specimen must be measured to fully document structural and mechanical properties.

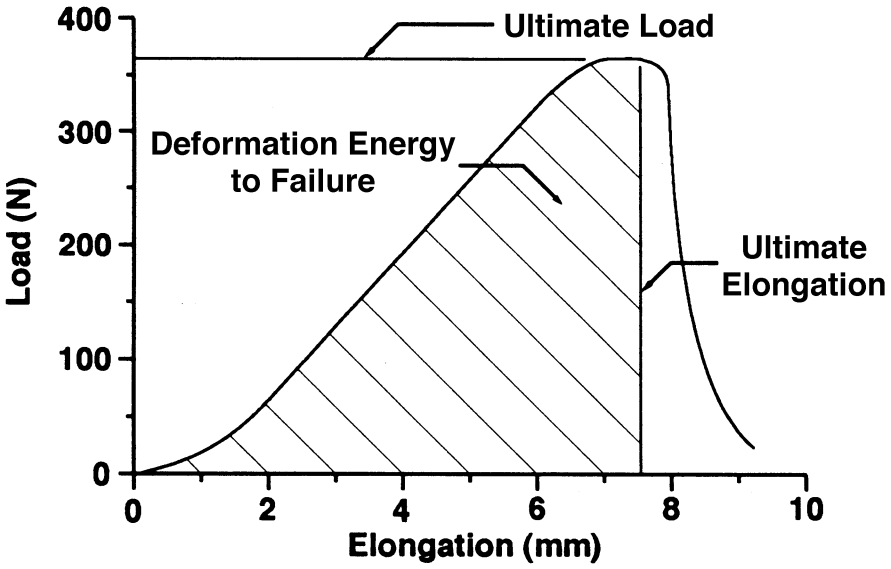

Figure A.2 Typical Load-Elongation Curve of Soft Tissue

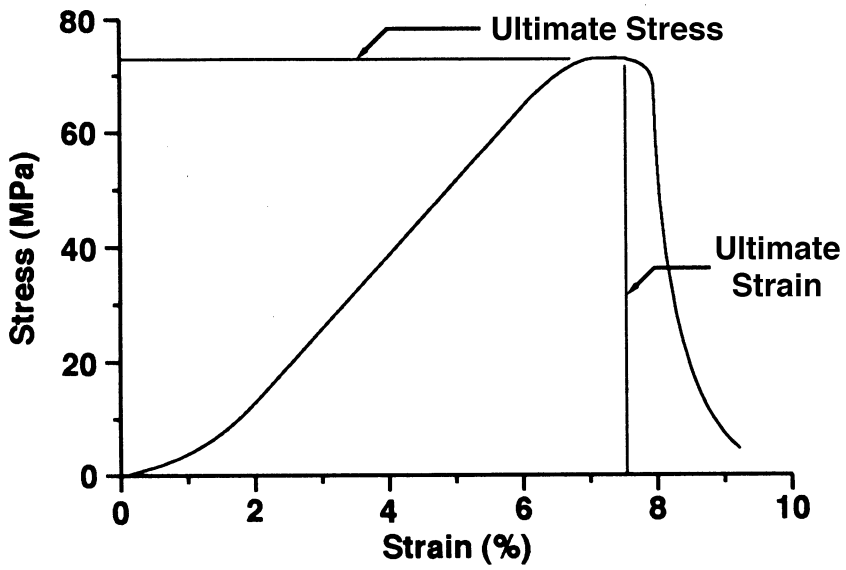

Figure A.3 Typical Stress-Strain Curve of Soft Tissue

A.2.1.1 Assessment of Cross-sectional Area

Many techniques have been used by researchers to determine the cross-sectional area of a soft tissue specimen [48,56]. One of the first approaches tried was the gravimetric method, in which the specimen's volume is calculated from its weight and then divided by its length to obtain the average cross-sectional area [17]. Because the cross-sectional area varies along the length of the

specimen, this approach can only produce approximate results. Furthermore, this method requires the researcher to know the density of the specimen.

Researchers have used several techniques to measure cross-sectional area that involve physical contact with the specimen [48,56]. One such method is based on the assumption that the specimen's cross-section is rectangular [48] or elliptical [29]. The length and width, or the major and minor axes, of the specimen are then measured with vernier calipers or a micrometer. For a tissue with a complex geometry, this method can lead to large errors [48]. Another method employs an area micrometer [13,19]. The specimen is compressed in a rectangular slot of known width, and the height of the tissue is measured with a micrometer. Allard et al. [1] showed that results from this method are sensitive to the pressure applied to the specimen. To determine the area of canine and swine medial collateral ligaments, Woo et al. [50] applied a minimal force to the specimen, used a cathetometer to measure the height, and assumed a rectangular cross-section. Researchers have also used a thickness caliper and a displacement transducer to determine the thickness profile across the width of a soft tissue specimen [44]. Deformation of the specimen as the thickness caliper was dragged across it may have led to large errors in this study [48,56].

To avoid errors due to distortion of the specimen during measurement, researchers developed noncontact methods to find cross-sectional area [48,56]. These procedures use optical means to determine the profile of a specimen. A rotating microscope [26], a video dimensional analyzer [40], and a laser beam [32] have all been used in this manner to achieve reasonable results. The principal drawback of these methods is the inability to identify concavities in the specimen surface, thus the result is always an upper bound of the area. To alleviate this problem, a system based on a laser reflectance transducer was developed [15]. The transducer emits a laser beam toward the specimen and collects reflected rediation from the specimen. In this way, concavities as well as complex shapes can be identified.

A.2.1.2 Assessment of Strain

Researchers have used various displacement transducers, including liquid metal gauges, Hall effect gauges, and differential variable reluctance transducers (DVRT) that involve direct contact with the specimen, as well as video-based noncontact methods to determine soft tissue strain [9]. Normalizing the displacement indicated by these transducers with respect to an initial length yields the tissue strain.

Liquid metal strain gauges consist of silastic tubing filled with mercury and sealed at each end with copper wire [12,33]. To measure tissue elongation, the tubing is aligned with the tissue fibers, and the copper wires are fixed in the bone at the insertion sites. A voltage applied to the copper wires across the gauge changes proportionately as the tubing is stretched. Liquid metal strain gauges are accurate to displacements of 0.2 mm [12].

The Hall effect transducer relies on a semiconductor that produces a voltage proportional to the strength of a magnetic field [6]. This semiconductor is fixed to one barb, and a permanent magnet is fixed to another barb. The arm of the permanent magnet is free to slide in the body of the transducer. The output voltage varies proportionally with the displacement of the magnet in the transducer and is linear in a range of 1 mm.

Beynnon et al. [10] implanted a DVRT to determine in vivo ACL strain. The DVRT consists of two coils and a sliding stainless steel core, which are attached to the specimen with barbs (Figure A.4). As the tissue elongates, the corresponding change in core position increases the reluctance of

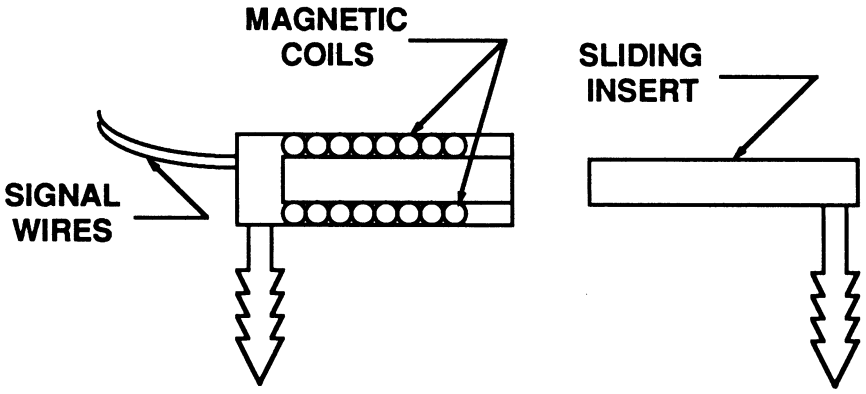

Figure A.4 Differential Variable Reluctance Transducer

one coil, while simultaneously decreasing the other coil's reluctance. Displacement output of the DVRT is linear in a range of 3 mm and is accurate to 0.001 mm.

Researchers developed the video dimension analyzer as a noncontact method to determine tissue strain [49,51]. In this technique, two or more lines are stained on the specimen perpendicular to the axis of loading to define the gauge length. The specimen is then videotaped while being loaded. The video signal during the playback of the videotape is routed through the video dimension analyzer, which converts the horizontal distance between the stain lines to a voltage. The voltage change over the duration of the test is related to the initial voltage to calculate tissue strain.

A.2.1.3 Anterior Cruciate Ligament

Researchers have studied the structural properties of the human femur-ACL-tibia complex (FATC), as well as that of rabbits, pigs, dogs, goats, and monkeys [47,48]. Noyes and Grood [39] found the stiffness of human FATC to be 182 N/mm, while Woo et al. [52] measured a stiffness of 242 N/mm. Reported values of human FATC ultimate load have ranged from 1725 N [37] to 2500 N [52].

Because of the complex structure, different portions of the ACL experience different levels of strain during loading [47]. Therefore, it is inappropriate to discuss the mechanical properties of the entire ACL, although researchers have examined the properties of individual bands (e.g. [54]).

A.2.1.3.1 Effects of Storage

The effects of storage on the structural properties of FATC have been examined by researchers [56]. No consistent changes in the structural properties of rabbit FATC were noted up to 96 hours postmortem [46], nor following storage at -20 °C for one week [45]. Noyes and Grood [39] detected no significant changes in the properties of monkey FATC stored for four weeks at -15 °C. Barad et al. [8] also found no significant changes in monkey FATC stored at -80 °C for three to five weeks, although a slight decreasing trend was noted.

A.2.1.3.2 Effects of Donor Age

Researchers have also studied the effects of donor age on the structural properties of human FATC [47]. Structural properties of specimens from young donors were two to three times those of specimens from older donors [39]. Woo et al. [56] reported similar results. However, these researchers presented conflicting reports of the effects of donor age on failure mode. In one study [39], specimens from young donors were more likely to fail in the midsubstance, while specimens from older donors were more likely to fail by bony avulsion. In the other study [56], the effects were reversed.

A.2.1.3.3 Effects of Flexion Angle

The angle of specimen knee flexion during testing has a significant effect on the structural properties of the FATC [20,53]. With increasing flexion angles, the ultimate load significantly decreased when loaded along the tibial axis, but did not when loaded along the ACL axis. Other structural properties followed similar patterns.

A.2.1.3.4 Effects of Strain Rate

Strain rate significantly affects the mechanical properties of the ACL [18] and the structural properties of the FATC [38]. Using a strain rate of 0.02%/s, Danto and Woo [18] found the modulus of rabbit ACL to be 711 MPa, versus 930 MPa when a strain rate of 381%/s was applied. Noyes et al. [38] found significant differences in maximum load, maximum strain, and energy absorbed to failure when elongation rates of 0.08 and 8.5 mm/s were applied to primate FATC.

A.2.1.3.5 Effects of Immobilization

The biomechanical properties of ligaments and ligament insertion sites are significantly affected by immobilization [55]. Researchers have reported decreases of about 25% in the ultimate load and stiffness of rat [31] and monkey [36] FATC after 4 and 8 week periods of immobilization, respectively. The effects of immobilization can be reversed through activity, although the process may be slow [55]. Following 8 weeks of immobilization, 12 months of activity was required to return the structural properties of the FATC to normal control levels [36]. However, Larsen et al. [31] found that only 6 weeks of activity were required to restore normal structural properties after 4 weeks of immobilization.

A.2.1.4 Patellar Tendon

Researchers have reported disparate values for structural properties of the central third of human patellar tendon. Cooper et al. [16] reported the ultimate load of 15 mm wide grafts to be 4389 N and that of 10 mm wide grafts to be 2977 N, while Noyes et al. [37] found the ultimate load of 14 mm wide grafts to be 2900 N. Cooper et al. measured the stiffness of 15 mm and 10 mm wide grafts to be 556 and 455 N/mm, respectively. Noyes et al. reported the stiffness of 14 mm wide grafts to be 685 N/mm. Because there were no significant differences in donor ages between the two studies, Cooper et al. suggested the discrepancy was because their clamp design reduced specimen slippage and decreased the occurrence of stress risers from crushing the specimen near the tendon insertion site.

A.2.1.4.1 Properties of Sections

The properties of sections along the length and width of patellar tendon have been investigated with varying results [14,23,37,57,59]. Compared to the middle region of the tendon, greater surface strains were noted near the bony insertion sites of human patellar tendon [14,59]. However, no significant differences in strain were seen between proximal, middle, and distal sections of rabbit patellar tendons [57]. Compared to the central region of the tendon, greater surface strains were noted by the edges [59]. Minimal variations in mechanical properties were seen between medial, central, and lateral sections of goat [23] and rabbit [57] patellar tendons. Similarly, no significant differences between the mechanical properties of medial and central sections of human patellar tendon were found [37].

A.2.1.4.2 Effects of Donor Age

Haut et al. [28] noted no significant differences in the mechanical properties of canine patellar tendon when considering effects of donor age. Similarly, Blevins et al. [11] found no significant effects of donor age on the mechanical properties of human patellar tendon. However, both of these studies calculated strain from grip-to-grip displacement, so the conclusions may be invalid.

A.2.1.4.3 Effects of Conditioning

Graf et al. [24] studied the viscoelastic response of primate patellar tendon and effects of conditioning the tissue. Specimens were conditioned either statically or cyclically, and then were allowed to recover for 60, 600, or 1800 s before being tested for stress relaxation responses at 2.5% strain for 10 minutes. Specimens conditioned statically at 2.5% strain for 10 minutes exhibited similar stress relaxation responses as specimens that were cyclically conditioned between 0% and 2.5% strain for 10 minutes. Effects of static conditioning were noted for all recovery times, although the effects were greatest with the shortest time.

A.2.1.4.4 Effects of Strain Rate

Researchers have examined the effect of strain rate on the structural and mechanical properties of patellar tendon [56]. Using strain rates of 0.02, 1.3, and 135%/s, Danto & Woo [18] found significant differences in the modulus of rabbit patellar tendon. The modulus determined using the fastest strain rate was 94% greater than when the slowest strain rate was used. Blevins et al. [11], on the other hand, found no significant differences in structural or mechanical properties of human patellar tendon subjected to strain rates of 10 and 100%/s. However, strain in this study was calculated from grip-to-grip displacement instead of from tissue elongation. Therefore, the calculated strain includes elongation of the insertion sites, which may confound interpretation of the results. Indeed, the modulus values from this study were 50% less than those reported by researchers that tested individual bundles of tendonous material [13]. Yamamoto et al. [57] demonstrated this effect when grip-to-grip displacement was incorrectly used to calculate strain. Strain rate did not affect the failure mode in any of these studies.

A.2.1.4.5 Effects of Twist

Cooper et al. [16] examined the effects of twisting the ends of a specimen on the structural properties of central third human patellar tendon grafts. Twisting the ends of the specimen 90° significantly increased the ultimate load and energy to failure of grafts of similar widths. Stiffness was not affected by the twist. No further differences were noted when the graft was twisted 180°.

A.2.1.4.6 Effects of Stress Shielding

Yamamoto et al. [58] reported that stress shielding significantly affects the structural and mechanical properties of rabbit patellar tendon. Using a stainless steel wire augmentation, the authors completely freed the patellar tendon from tension. Changes in properties were noted as little as 1 week postoperative. During the first 3 weeks postoperative, the tensile strength, modulus, and ultimate load of the specimen decreased to 9%, 9%, and 20% of controls, respectively. Stiffness of the specimen was not reported. However, between 3 and 6 weeks postoperative, the properties tended to increase. The authors provided no explanation for this trend.

A.2.2 Biochemical Properties

The protein collagen comprises most of the dry weight of connective tissues and contributes significantly to their biomechanical properties [2]. Although 16 types of collagen exist in humans, tendons and ligaments contain primarily Types I and III [7]. Research identifying the collagen content of the ACL and the patellar tendon is reviewed.

A.2.2.1 Anterior Cruciate Ligament

The collagen content of the ACL is 86% to 90% Type I and 10% to 14% Type III [3,5]. Researchers have shown that the collagen fibrils of human ACL conform to a bimodal profile with respect to diameter size [21,42,43]. The diameter of a majority of fibrils lies within the 30 to 100 nm range, although some fibrils are greater than 100 nm in diameter. The diameter profile changes with age [43]. At birth, the profile is unimodal with small diameter fibrils. The fibril diameter increases until physical maturity, at which point the profile becomes bimodal. The fibril diameter decreases with further aging.

A.2.2.2 Patellar Tendon

The collagen content of patellar tendon is greater than 95% Type I and less than 5% Type III [3,5]. The collagen fibrils of patellar tendon form a population that is markedly different from that of the ACL [41]. Approximately 45% of the fibrils have a diameter that is greater than 100 nm.

A.2.3 Histological Properties

Histological analysis of connective tissue involves the description of two variables: (a) cell morphology and size and (b) the regular sinusoidal pattern in the extracellular matrix, called the crimp. Literature describing these variables in the ACL and the patellar tendon is reviewed.

A.2.3.1 Anterior Cruciate Ligament

The shape of fibroblasts in the ACL ranges from ovoid to fusiform. Whether these cells form one population, or several, is not known, because researchers describe cells from a variety of species. The effects of skeletal maturity, mechanical stress, and donor site location on cell shape are not understood. The ovoid fibroblasts are arranged in columns between collagen fibers, while the fusiform cells are typically distributed throughout the midsubstance of the ACL. However, a clear distribution pattern has not been described in any species. Amiel and Kleiner [4] studied the crimp in rabbit ACL, and measured an amplitude of less than 5 μm and a period of 45-60 μm.

A.2.3.2 Patellar Tendon

Patellar tendon is histologically a more uniform tissue than the ACL. Amiel and Kleiner [4] identified spindle shaped fibroblasts aligned longitudinally in rabbit patellar tendon. Collagen bundles approximately 20 μm in diameter were also aligned longitudinally [2]. The crimp amplitude was measured as 15 μm, and the period was 120 μm.